Correlation of Near-infrared (NIR) Spectroscopy with Water Quality Sensors to Detect Concentration of *Saccharomyces boulardii* in Water

Muhammad Aqil Hafizzan Nordin[a], Mohd Faizal Jamlos[a,b], Siti Anis Dalila Muhammad Zahir[a], Mas Ira Syafila Mohd Hilmi Tan[a], Hajar Fauzan Ahmad[c], Mohd Aminudin Jamlos[d], Nor Husna Mat Hussin[c]

[a] *Faculty of Electrical & Electronics Engineering Technology, University Malaysia Pahang, 26600, Pekan, Malaysia*
[b] *Centre of Excellence for Artificial Intelligence & Data Science, Universiti Malaysia Pahang, 26300, Gambang, Malaysia*
[c] *Faculty of Industrial Sciences and Technology, University Malaysia Pahang, 26300, Gambang, Malaysia*
[d] *Faculty of Electronic Engineering & Technology, Universiti Malaysia Perlis, Arau, 02600, Malaysia*

ABSTRACT

Terahertz (THz) sensing of high sensitivity detection has given the possibility of a non-invasive method for measuring and monitoring microorganism from water resources. The purpose of this study is to analyse the effectiveness of Near-infrared (NIR) spectroscopy as a non-destructive and in-situ measurement-based method for detection of *Saccharomyces boulardii (S. boulardii)* in water. Samplings are prepared in biotechnology lab in Universiti Malaysia Pahang (UMP), a yeast species of *S. boulardii* is used as a model microorganism. A single colony of yeast was inoculated in liquid broth media and incubated for overnight culture. A standard serial dilution method was applied to prepare five samples at different yeast concentration in corresponding test tubes of 0%, 10%, 20%, 50% and 100%. A hand-held NIR spectroscopy with range from 900nm to 1700nm wavelength is deployed gapless to scan those test tubes through its optical window. Meanwhile another sample with similar concentrations are inoculated into volume 0.0071 m³ of water equipped with water quality sensor system for monitoring and analysis purpose. The findings show inoculation certain concentration of 10%, 20%, 50% and 100% of *S. boulardii* into the water generated certain level of NIR spectroscopy's spectral absorbance of 0.723, 0.64, 0.357 and 0.121 correspondingly at 1067 nm wavelength. This proves NIR spectroscopy is a highly-sensitivity THz sensor at 1067 nm wavelength as absorbance is at the minimum level as *S. boulardii* concentration is at the maximum. This finding is further validated by Dissolved Oxygen (DO) sensor which demonstrates rising maximum of 8 ppm after an hour of *S. boulardii*'s inoculation compared to 4 ppm in a normal water. However, the DO level back to normal after 5 hours due to the acclimatization process of the yeast and demonstrate capability of DO sensor to detect presence of yeast in water. PCA and PLS analysis based NIR spectroscopy's spectral absorbance also demonstrates ability to categorise severity of a microbial illness depending on its concentration. The results from this study has suggested that the NIR spectroscopy sensor as an excellent option for microbial sensing in water.

Keywords: yeast; *Saccharomyces boulardii*; Near-infrared spectroscopy; Internet-of-Things (IoT)

1. Introduction

Timely and precise microbial detection is crucial for numerous health and safety applications, which stimulates the continued development of adaptable optical sensors for microbial investigations [1]. THz frequency ranges have the potential to be used in the fabrication of extremely sensitive and selective microbial sensors capable of rapid on-site detection of microbes in both ambient and aquatic conditions. THz can find very small amounts of microbes because their sizes are similar to the size of the tiny gaps in THz frequencies [2]. In contrast to other approaches like measuring the water potential of the leaves or comparing their fresh and dry weight, THz and sub-THz measurements have benefit of being a non-invasive procedure. This implies that repeated measurements on the same sample over a short period of time are achievable without need for laboratory procedures [3]. THz sensing is widely used in agriculture sector to evaluate product quality by measuring protein and fat content, as well as in textile, polymer, and petrochemical industries [4]. Biomedical sector even deployed THz technology including NIR spectroscopy for skin and dental diagnostics imaging [5]-[6].

Table 1. Methods for bacteria detection.

Bacteria Detection Methods			
Serological methods	**Molecular methods**	**Biomarker-based sensor**	**Remote sensing**
Flow cytometry [7]	Fluorescence in-situ hybridisation (FISH) [10]	Gaseous metabolite profiling [13]	Imaging technique [15]
Enzyme-linked immunosorbent assay (ELISA) [8]	Polymerase chain reaction (PCR) [11]	Water metabolite profiling [14]	Spectroscopy technique [16]
Immuno-fluorescence [9]	DNA arrays [12]		Metamaterial technique [17]

NIR spectroscopy sensor has features of in-situ, label-free, non-invasive and non-destructive analysis of chemical and biological compounds [18]. Thus, the NIR sensor recently emerged as a potential approach for serological, molecular, and biomarker-based sensor as shown in Table 1. NIR spectroscopy within wavelength of 700-2500nm to biological samples based on reflected spectral have drawn lots of attention among researchers e.g. microbiology for multivariate classification of microbial detection [19]-[20] and detection of microorganisms such as fungus, bacteria, and viruses in water, food and human [21]-[22]. A million bacterial cells can be found in a millilitre of fresh water. Microbes come in a variety of shapes and sizes where shape is one of method to categorise

them. For example, there are three primary shapes to be aware of, spherical, rod and spiral shapes of bacteria [23]. Bacteria size is about $\sim\lambda/100$, resulting in a small scattering cross-section to the NIR's wavelength of 700-2500nm to trigger unique spectrum sensitivities based on shape, size and concentration [24]. Fig. 1 shows the spectra's absorbance of *Escherichia coli* (*E. coli*) and *Klebsiella pneumoniae* (*K. pneumoniae*) strains to distinguish between carbapenem-resistant (CR) and susceptible strains. The presence *E. coli* and *K. pneumoniae* can be seen over the wavelength between 700 and 2350 nm but the vibration at particular wavelength to distinguish between the two bacteria are too random and unsynchronized might be due to different in concentration since both of them are in a rod-shaped [25].
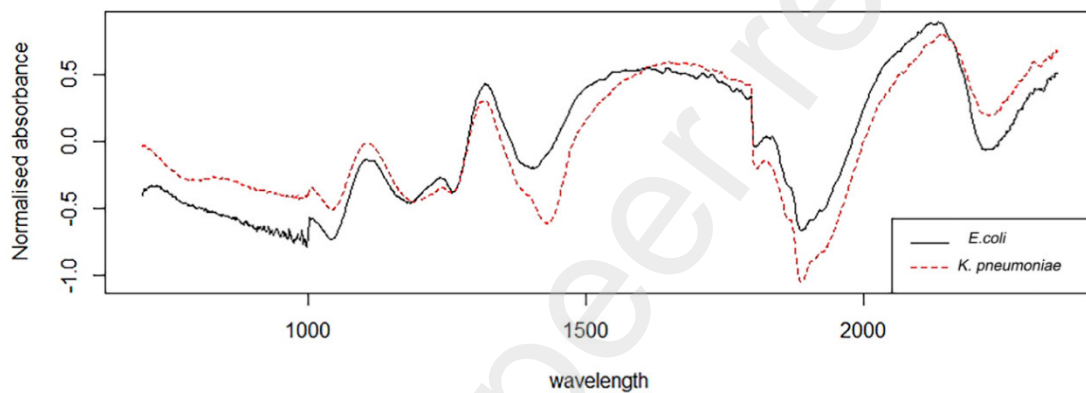
Fig. 1 Normalized absorbance of *E. coli* and *K. pneumoniae* between 700 and 2350 nm [25] (in the figure put the starting value (0 and 3000 for wavelength axial)

To date, an advanced method based on sequencing allows precise microbial identification across microbial kingdoms from various microenvironment settings [26-29], but very laborious and less timely to be deployed in situ. However, NIR spectroscopy has potential to design as a software sensor (soft sensor) for particular application in term of accuracy and rapidness using *Saccharomyces boulardii* (*S. boulardii*) as fungi detection model. Soft sensor could be a cost-effective solution to virtually monitor the concentration of bacteria in wastewater and to optimize disinfectant dosage accordingly. In the past few years, researchers have looked into how NIR could be used to find and identify bacterial and fungal pollutants in various environments and medium. Ref. [30] evaluated the use of NIR for detecting and identifying bacterial and fungal contaminants in food. The authors discovered that NIR correctly detected a broad variety of bacterial and fungal pollutants, such as *Salmonella, E. coli*, and *Staphylococcus aureus* (*S. aureus*). They also discovered that NIR could identify fungal pollutants, including *Aspergillus*, *Penicillium*, and *Fusarium*. Anal et. al. journal investigated the use of NIR for detecting bacterial and fungal strains samples in the air. NIR has

correctly identified a wide range of bacterial and fungal species, like *Pseudomonas*, *Staphylococcus* and *Candida*. Meanwhile ref. [31] deployed NIR as data collector tools in suppling input to multivariate analysis software for distinguishing between various bacterial strains. The NIR with multivariate analysis correctly identified a broad variety of bacterial strains such as *E. coli*, *S. aureus*, and *Pseudomonas aeruginosa* (*P. aeruginosa*). NIR spectroscopy and chemometrics in categorising bacterial and fungal strains have been discovered by ref. [32-34]. The authors discovered that NIR spectroscopy and chemometrics correctly classified bacterial and fungal species of *Bacillus subtilis*, *Streptococcus pneumoniae* and *Aspergillus niger*, *E. coli*, *S. aureus* and *Candida albicans*.

Table 2. Summarizes on NIR methods for detecting bacteria.

Ref(s)	Method	Findings Bacteria
[30]	NIR	*Salmonella, E. coli, S. aureus, Aspergillus, Penicillium, Fusarium.*
[31]	NIR	*Pseudomonas, Staphylococcus, Candida.*
[32]	NIR + Multivariate Analysis	*E. coli, S. aureus, P. aeruginosa.*
[33]	NIR + Chemometrics	*Bacillus subtilis, Streptococcus pneumoniae, Aspergillus niger.*
[34]	NIR + Multivariate Analysis	*E. coli, S. aureus, Candida albicans.*

In overall, table 2 illustrates the potential of NIR spectroscopy for detecting and identifying bacterial and fungal contaminants in food items, environmental samples, and clinical samples. None of them however have classified neither NIR's absorbance, transmittance nor reflectance of those bacteria based on the concentration. It is worth noting that only certain concentration of bacteria could bring the harm to living creatures include human and animal. In this paper, a hand-held NIR spectroscopy with range from 900nm to 1700nm wavelength is deployed to scan certain concentrations of yeast in water which generated certain level of NIR spectroscopy's spectral absorbance. The study found discrepancies of absorbances' spectral at particular 1067 nm wavelength reflecting the detection of *S. boulardii* yeast concentrations which further validated by DO sensor. It has been notified that DO provide the spike with the immediate presence of 50% and 100% concentration of *S. boulardii* compared to other water quality parameters such as pH and

Electrical Conductivity (EC). Such correlation between the NIR spectroscopy and DO sensor have never been discussed and disclosed previously. The paper is organized as follows. Section 2 presents the detail of the sample preparation and system process development. Section 3 presents results and discussion. Lastly, Section 5 presents the conclusion and limitations of the study.

2. Methodology

The dataset and proposed methodology have been discussed in detail in this section.

### 2.1 Sample Preparations of *S. boulardii* Culture and Serial Dilution

For media preparation, 40 g of Sabouraud Dextrose Agar (Sigma-Aldrich, USA) was dissolved in 1 L of distilled water, and sterilized by autoclaving at 121°C for 15 minutes. The agar was allowed to cool to 50 °C and poured into sterile Petri dishes to let the agar solidify. A yeast strain of *S. boulardii* UMP2109 was inoculated from a frozen storage by streaking the yeast onto the surface of the agar with a sterile loop aseptically with minor modification. The plates was incubated at 30°C for 18 to 24 hours and white or cream-colored colonies were observed on the agar as shown in Fig.2.

Fig.2 The formation of white colonies of *S. boulardii* UMP2109 on Sabouraud Dextrose Agar media after 18 hours of incubation.

Next, a *S. boulardii* UMP2109 single colony was inoculated to Sabouraud broth to allow it to grow and multiply. Briefly, Sabouraud broth was prepared by dissolving 40 g of Sabouraud media in 1 L of distilled water and sterilized by autoclaving at standard parameters. Once the Sabouraud broth cooled to room temperature, a single colony of *S. boulardii* UMP2109 was picked from the Sabouraud agar plate and transferred the colony into a broth. The broth and the colony was mixed by gently swirling prior incubation at 30°C for 18 to 24 hours. After incubation, the vials were examined for the presence of *S. boulardii* growth by observing the changes of broth turbidity.

Then, a four-time serial dilution was carried out. Six vials were prepared, for which the first vial (labelled as 100%) was an original culture from an overnight culture, and 9 ml of sterile, distilled water was made and placed in each of the other five vials Fig.3. Labels on the vials read 5X (1:10), 2X (1:100), 1X (1:1000), 0.5X (1:10,000), and B (1:100,000). First, 9 ml of sterile, distilled water were added to the second vial marked 5X to achieve 1:10 dilution factor along with 1 ml of the original culture sample. As a result, the initial culture sample was 10 times more diluted. Second, 1 ml of the 1:10 solution was added to the 2X vial to achieve 1:100 solution, and well mixed. Then, in the vial marked 1X, 9 ml of sterile distilled water were added to 1 ml of the solution from the vial 2X. The fourth vial, marked 1X, was then filled with 1 ml of the solution from the 2X vial to achieve 1:1000 dilution. A 10,000 fold dilution factor was used to dilute the solution in fifth vial labelled as 0.5X. Finally, the sixth vial, marked B, was then filled with 1 ml of the solution from test tube 0.5X to achieve 1:100,000. These vials were further used to be analysed in the next step.
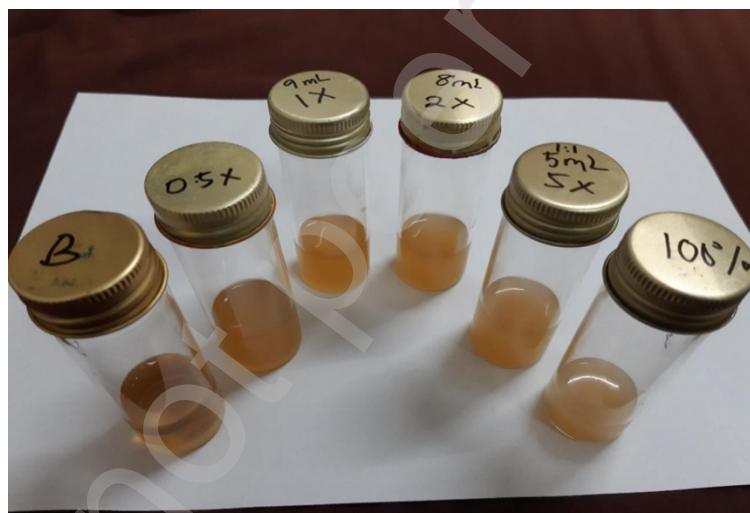

Fig.3 The samples *S. boulardii* yeast via serial dilution.

2.2 Data collection by DLP NIR spectroscopy

DLP NIRscan Nano spectrometer (DLP2010NIR DLP® NIRscan™ Light) with a measurement range of 900–1700 nm (176–333 THz) is deployed to collect the NIR's spectral reflectance and absorbance. Fig. 4 (a) shows the DLP NIRScan NANO as a tiny, portable, and highly adjustable device for performing near-infrared (NIR) spectroscopic studies on materials sampling. The DLP NIRScan Nano uses the latest DLP technology to improve spectral resolution, optical throughput and sensitivity while reducing system size and maximise measurement functionality and flexibility. Spectroscopy is a method of measurement investigating material's characteristics by observing how it interacts with light at various wavelengths. The material is not harmed, destroyed, or transformed

during measuring process, hence this information is collected non-destructively. Absorption, reflection, and emission of light by the materials are all examples of interactions that could be measured.


(a)　　　　　　　　　　　　　　　　　　(b)
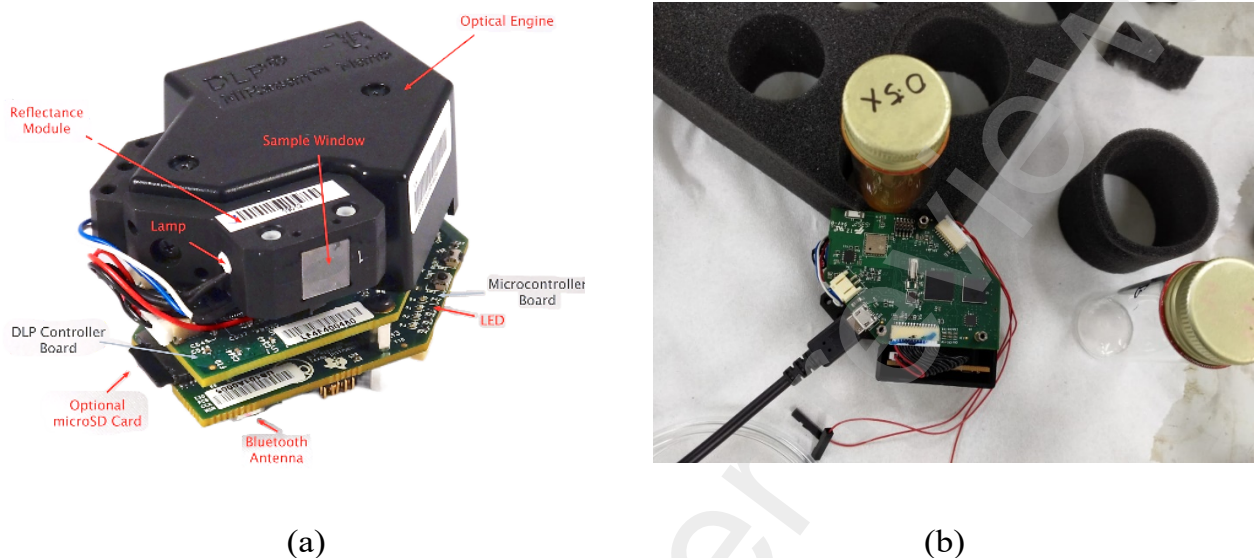
**Fig. 4** (a) DLP NIRscan Nano spectrometer (b) Data Scanning of *S. boulardii*

Three different parameters which are intensity, absorbance and reflectance are provided when the DLP NIR spectrometer finished scanning. Fig. 4 (b) shows NIR spectroscopy is deployed gapless to scan the test tubes through its window. The test tubes with certain concentration of *S. boulardii* are shown in Fig.4. The amount of light energy absorbed and the wavelength at which it is absorbed may both be used to define a material. The degree of absorption is determined by the concentration of the components inside the substance.

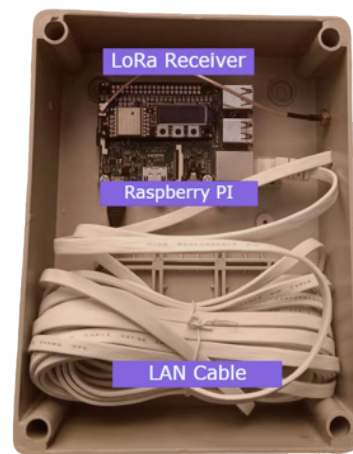## 2.3 IoT based Sensors for Water Quality Measurements

The idea to develop IoT based sensor system is to correlate and investigate the concentration effect of *S. boulardii* over few sensors which is very much related to the water quality parameters such as pH, DO, EC, TDS temperature and range. Fig. 5(a) represents block diagram of the IoT based sensors system consisted of pH, DO, EC, TDS temperature and range sensor. The prototype of IoT based sensors system is comprised of pH, DO, EC, TDS, temperature and range sensor, as depicted by Fig. 5(b) and (c) and Lora have been deployed as wireless module to send the data of sensors wirelessly to Gateway (GU). The reading of pH, DO, EC, temperature and range are stored into SQL database after the decoding process using LAMP server.
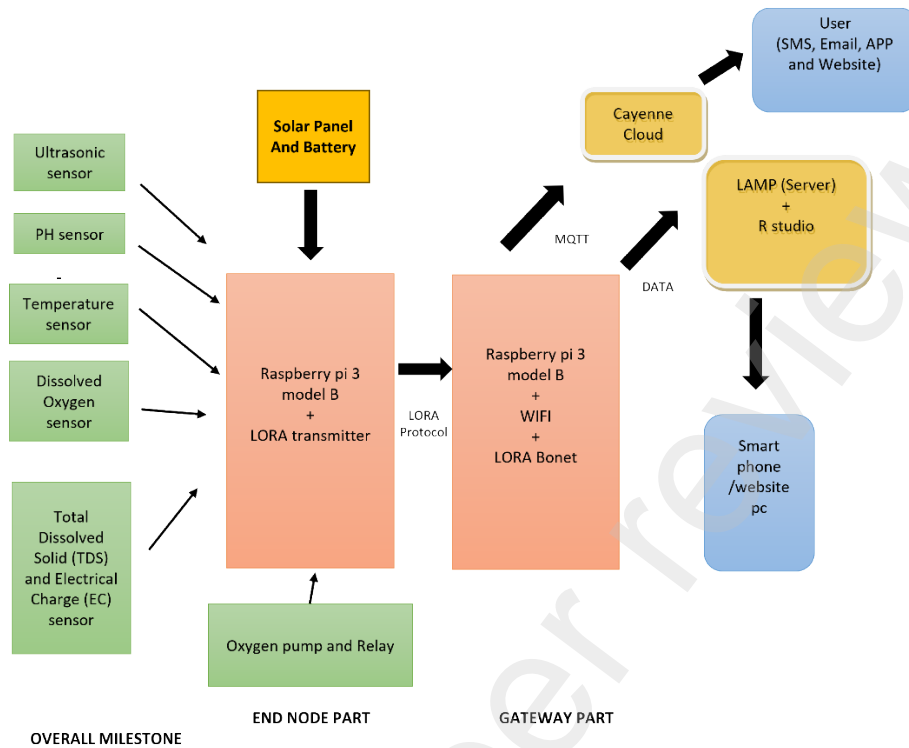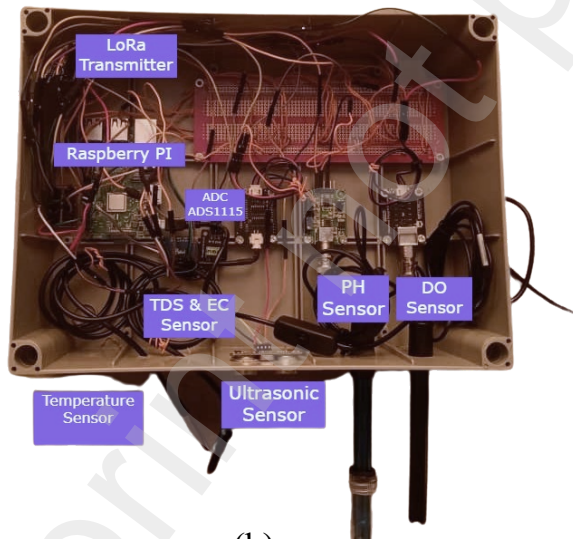
Fig. 5 Water Quality Measurement device a) System flow diagram b) IoT based sensor c) Gateway (GU)

The same samples of Fig. 3 have been poured into aquarium, one at a time based on certain concentration. The aquarium is fixed with IoT based sensor system as shown in Fig. 6. Each sample

is tested by monitoring all parameters every one hour e.g. 50% concentration of *S. boulardii* is poured into the aquarium and those sensors will send the data to GU and server for every one hour. The discrepancy of data will be observed in details to determine the impact of yeast on each water quality parameter. The server environment window for sensors data display including date and time can be seen in Table 3.

(a)   (b)

Fig. 6 (a) Single sensor detection (b) Multi sensors detection in aquarium

Table 3. Data water quality measurement

| IOT WATER QUALITY PARAMETER					
DATA					
Date	TDS (ppm)	EC (mS/cm)	PH	DO (mg/L)	TEMP (ºC)	WATER LEVEL(CM)
25/4/2022 23:37	259.119	1.55472	7.23449	4.448	28.937	10
25/4/2022 23:16	266.184	1.5971	7.21253	3.36	28.937	11
25/4/2022 22:01	258.833	1.553	7.04698	5.712	29.062	9
25/4/2022 19:12	258.833	1.553	7.04698	5.712	29.062	9
25/4/2022 18:45	262.157	1.57294	7.07063	5.728	28.875	9
25/4/2022 17:01	242.532	1.45519	7.06894	6.288	28.812	10
25/4/2022 14:16	242.532	1.45519	7.06894	6.288	28.812	10
25/4/2022 14:02	245.744	1.47446	7.05205	7.504	28.437	10
25/4/2022 11:32	245.744	1.47446	7.05205	7.504	28.437	10
25/4/2022 11:31	247.51	1.48506	7.06725	7.584	28.437	10
25/4/2022 11:30	247.198	1.48319	7.04022	7.824	28.562	10
25/4/2022 11:28	245.293	1.47176	7.0588	4.896	28.5	10
25/4/2022 11:01	238.155	1.42893	7.15003	4.608	28.375	10
25/4/2022 9:01	238.155	1.42893	7.15003	4.608	28.375	10

3. Results and discussions

This section has been divided into few subsections according to certain analysis. 3.1 explained on absorbance and intensity spectral collected by NIR spectroscopy while 3.2 discussed findings from IoT based sensors system. Subsection 3.3 reflected to analysis of PCA and PLS operation with NIR spectroscopy method while SVR operation for DO sensor. Correlation finding of NIR spectroscopy and DO sensor is described in subsection 3.4.

3.1 NIR Absorbance

Fig. 7 shows spectral absorbance of *S. boulardii* to reflect interaction of the light absorbance across the NIR's wavelength between 900 and 1700 nm. Patterns based on absorbances' concentration spectral are observed and identified as concentration of yeast increases, the absorbance decreases from wavelength of 980 to 1150nm, related to a higher concentration of CH3. Meanwhile absorbance increases from 1350nm to 1550nm due to greater intensity of oxygen and hydrogen. Fig. 7(a) reflects the increases concentration from 10%, 20%, 50% up to 100% of yeast lead to the absorbance synchronizing reduced correspondingly from 0.723, 0.64, 0.357 to 0.121 at 1067nm wavelength. This demonstrates that NIR spectroscopy at 1067 nm wavelength is a soft THz sensor for detecting microbe concentration in water. It is observed as well concentration of 0% and 0.5% have constantly levelled at ≈ 0.7- 0.8 absorbance spectral as in Fig. 7(b), which replicated as a normal water. The finding suggests that NIR spectroscopy's absorbance spectral considered as insufficient to identify concentration of *S. boulardii* less than 10% concentration which is overall shown by Fig. 7(c).

(a)

## Absorbance

(b)

Absorbance

(c)
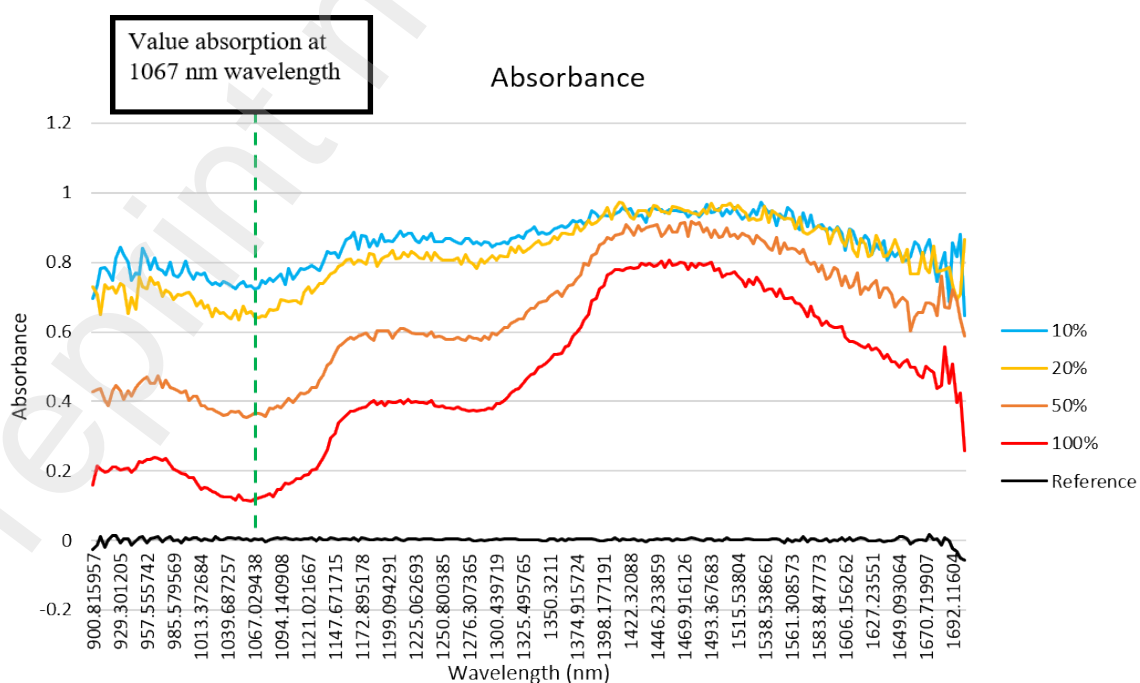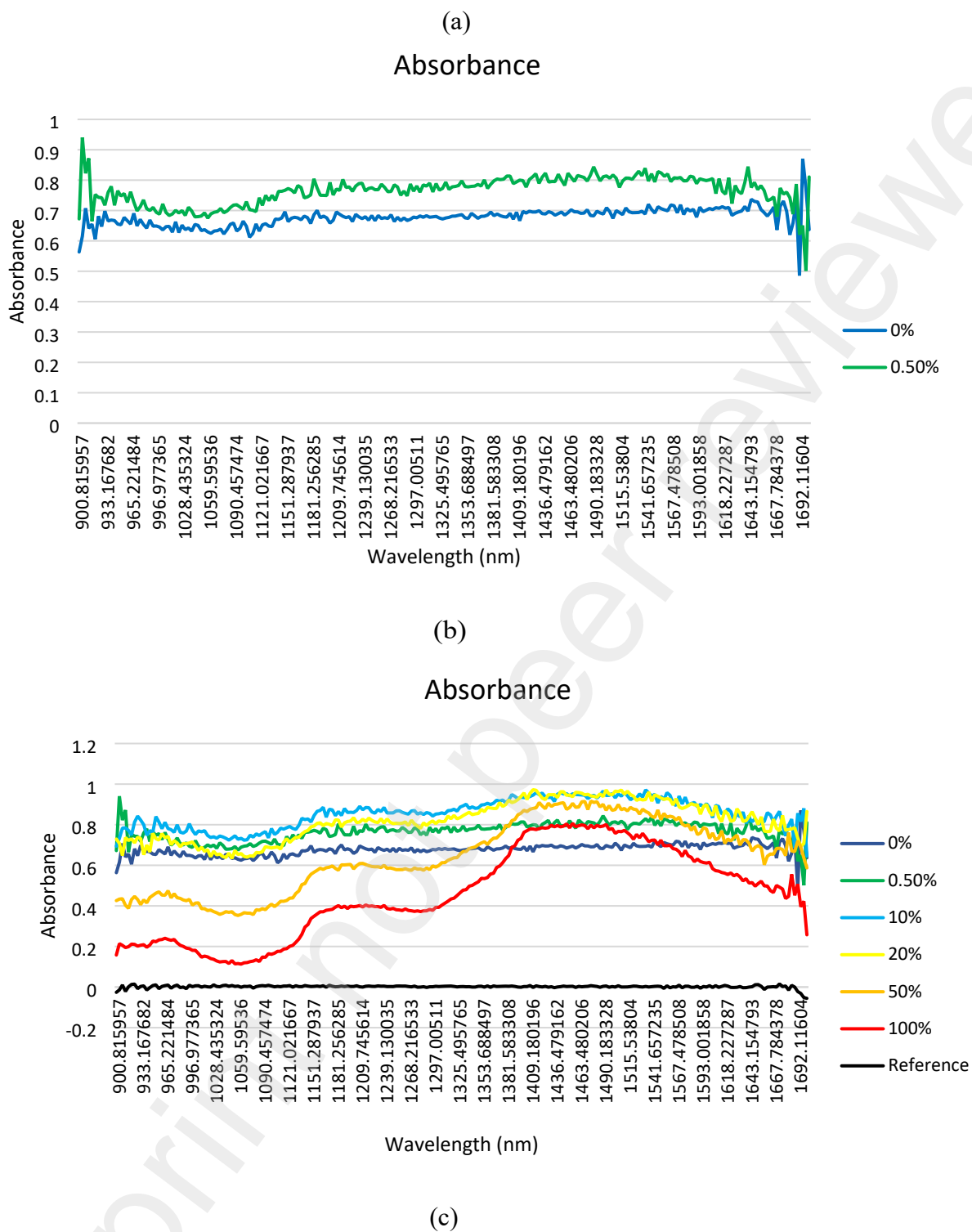
Fig. 7 Absorbance spectral data based on concentration (a) 10%, 20%, 50%, and 100% (b) 0% and 0.5% (c)

Absorption spectrum is derived by dividing the incoming light to the intensity spectrum. Thus, instead of absorbance, intensity as substantial data accessible of chemical information on the samples, especially how much they are concentrated compared to the other samples as shown in Fig.

8. The intensity raw data of the samples are skewed and no obvious discrepancies between concentrations, see Fig. 8(a). By normalising the data, a clear pattern of concentration-based detection of *S. boulardii* can be seen over the wavelength of 1070nm. The intensity increases as concentration increases. Meanwhile, an opposite pattern of intensity is observed starting from 1350nm to 1550nm.
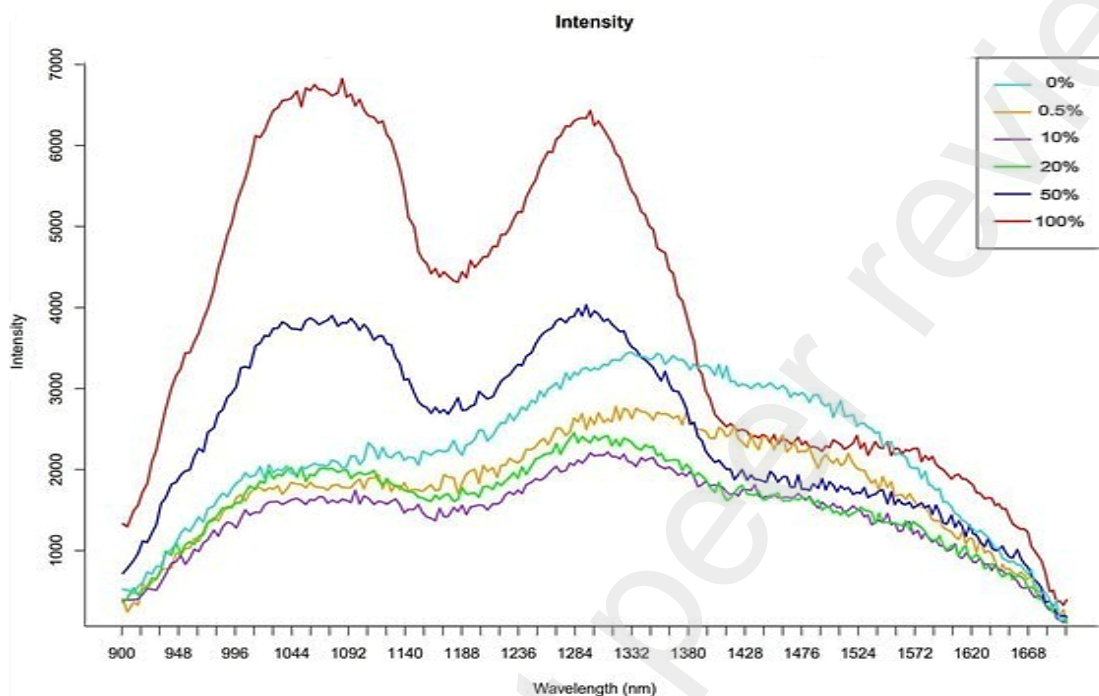
(a)
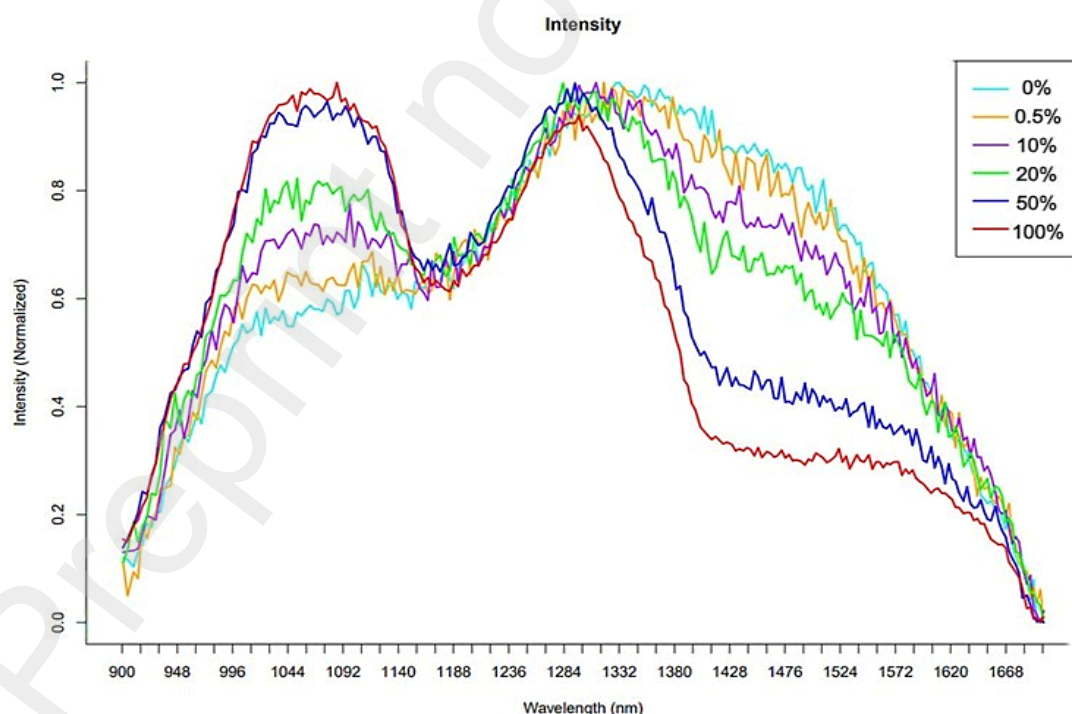
(b)

Fig. 8 Intensity spectral data (a) raw data (b) normalized data

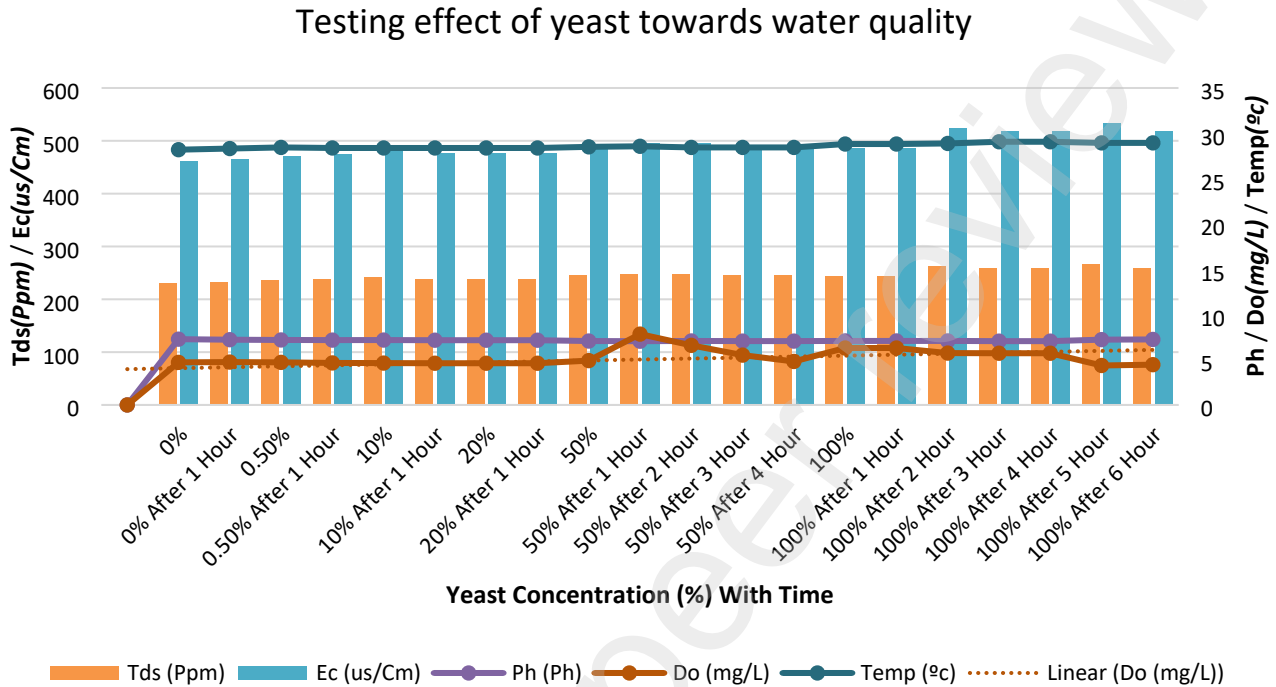### 3.2 IoT based Sensors System reacted to different Concentration of S. boulardii yeast

Fig. 9 Reaction of sensors to different concentrations of S. boulardii

As mentioned in section 2.3, IoT based sensors system able to sense five parameters of water quality measurement with all sensors simultaneously dipped into different concentration samples of *S. boulardii* for analysis purpose. Fig. 9 shows DO have been fluctuated compared to other parameters such as EC, pH and TDS for the sampling of 50% and 100% concentration. DO reading increases after an hour sampling poured into aquarium, and it is observed DO returned to its original value of 4 mg/l after 4 hours. DO have increased to the range of 8mg/l and then back to normal at 4 mg/l due to the bacteria died after few hours of poor water quality. As the concentration increase, the yeast depleted more oxygen content in the culture medium. At certain point, this depletion affected and starting to harm those yeast. Fig. 10 scrutinized the DO condition when concentration transited from 50% to 100%. 50% sampling taken up to 4 hours to normalize the DO from 7.824 mg/l to 4.804 mg/l while 100% sampling dragged longer of 6 hours to normalize it from 6.288mg/l to 4.36mg/l. This is due to the acclimatization process which refer to the physiological adaptations of those yeast.Fig. 10 has demonstrated sensitivity of DO sensor to detect the presence of *S. boulardii* only when concentration reached 50% and above.
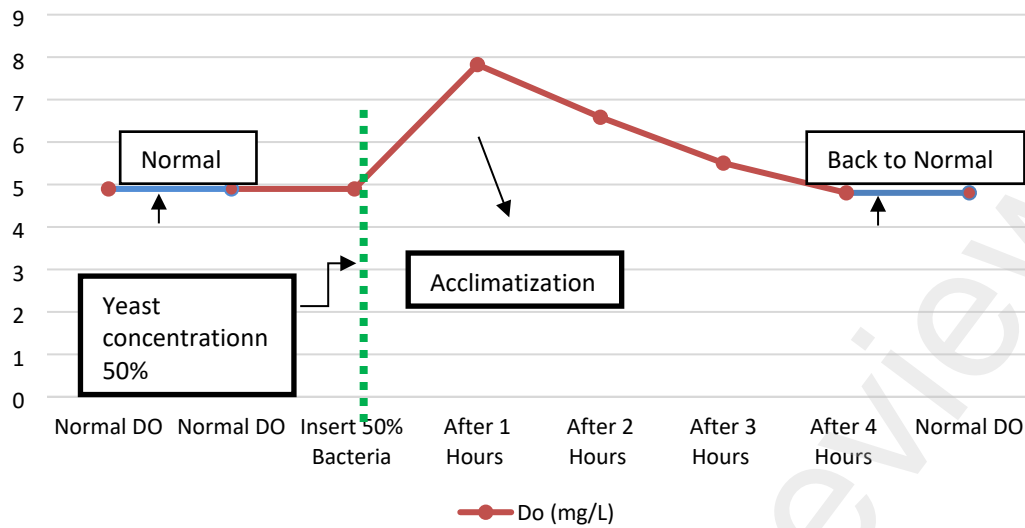
(a)
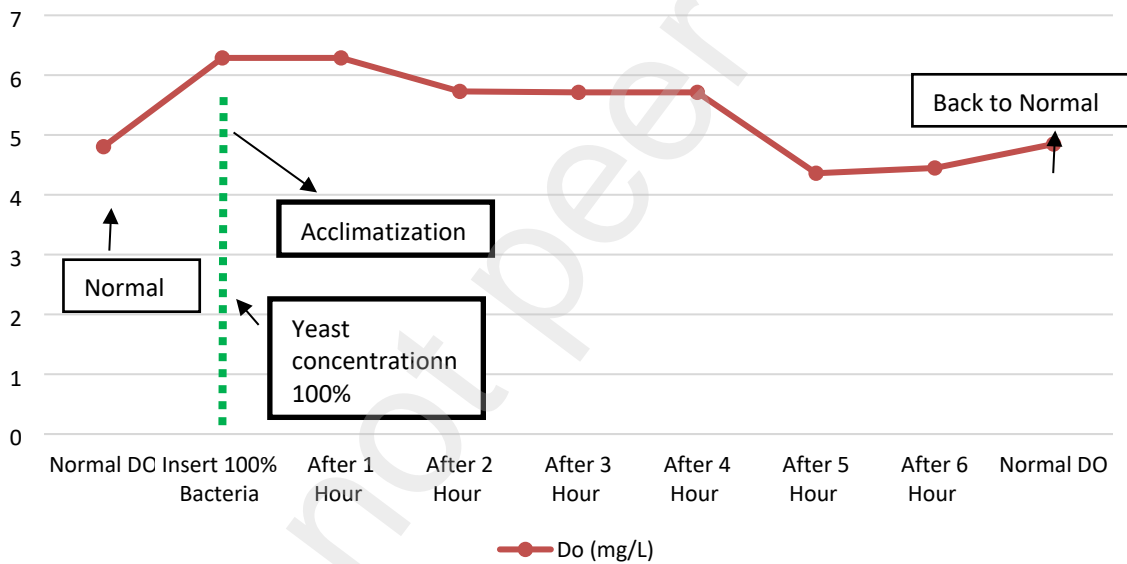
(b)

Fig. 10. Chart of effect dissolved oxygen to yeast sample 50% and 100%

3.4 PCA and PLS Analysis for NIR spectroscopy method.

Principal Component Analysis (PCA) and Partial Least Squares (PLS) are deployed to further analyse the obtained NIR spectroscopy data. PCA is designed to decrease complexity of data by identifying patterns and trends while PLS provides a statistical prediction model for monitoring concentration of microorganisms. Variance calibration model and 3D score plot analysis have been deployed to identify numbers of group principle components (PC) especially if it is involved with more than two relevant PCs.

Fig. 11(a) shows 3D score plot is constructed by PC-1, PC-2, and PC-3, and the blue points indicate the data of microbial concentrations (0%, 0.5%, 10%, 20%, 50%, and 100%). Correlation between concentrations and the PCs are represented by the location of the data points. Concentrations of *S. boulardii* which more comparable are closer together while those that are further away are less similar. The figure listed three main components (PC-1, PC-2, and PC-3) and the scores which correlate to various microbial concentrations, where 0 denotes 0%, 0.005 represents 0.5%, 0.1 denotes 10%, 0.2 denotes 20%, 0.5 denotes 50%, and 1 denotes 100%. Based on Fig. 11(a), first principal component (PC1) had explained the most variance of the data while second principal component as the second-most variation (PC2) which are levelled at 93% and 7% correspondingly. This indicates that the bulk of the information included in NIR spectral data is focused on PC-1, whereas PC-2 includes less important or redundant information. PC-1 and PC-2 scores change noticeably when the microbial concentration rises. This change may indicate that these two major factors are linked to the presence of microbial in the sample.

(a)   (b)
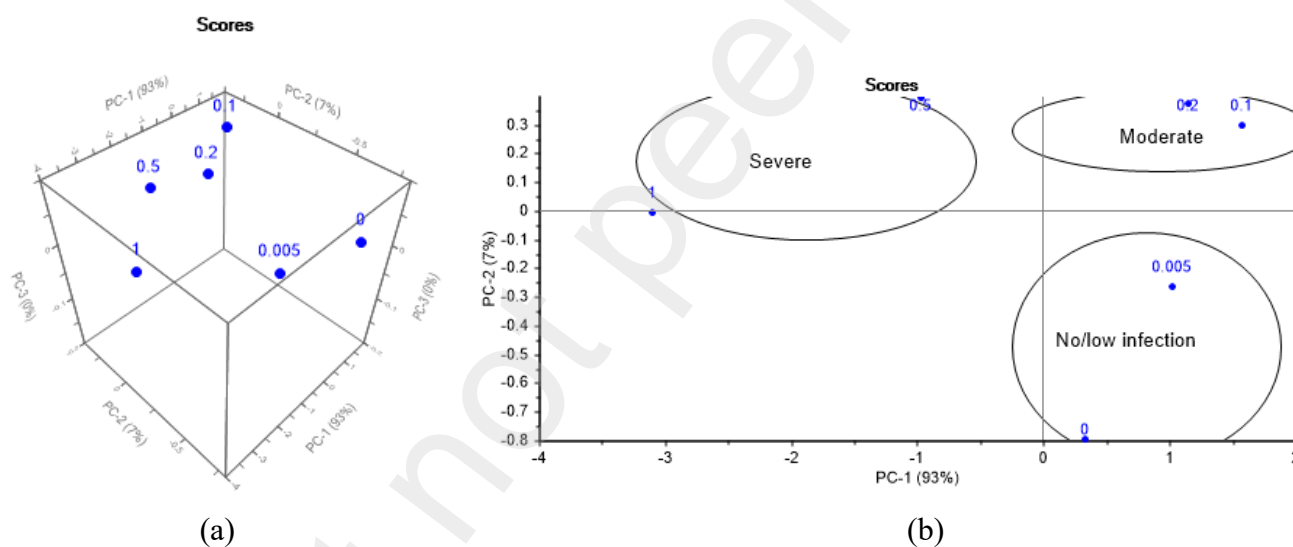
Fig. 11 PCA analysis based on certain concentration (a) Different concentrations based on 3D score plot (b) Analysis on PCs concentration

In contrast to PC-2, PC-1 clearly distinguishes between low and high microbial concentrations. On the other hand, PC-3 seems to have significant effect on the concentration. Based on PCA analysis, it is found that low, moderate, and high microbial concentrations may be distinguished using the PC-1 and PC-2 scores. These results could be helpful for microbials' detection and classification. To simplify the study, each concentration represents certain severity level as 0% and 0.5% considered as no or low-infection, 10% and 20% for moderate infection, and 50% to 100% having a severe infection, as shown in Fig. 11(b). PC-1 and PC-2 is observed in a scattered diagram, allowing to see the distribution of severity levels easily. The no- or low-infection group (0 and 0.5%)

found to have positive PC-1 values and negative PC-2 values while moderate (10% to 20%) had both positive on PC-1 and PC-2. However severe infection (50% to 100%) has negative PC-1 values and positive PC-2 values. This finding demonstrates that PCA able to categorise severity of a microbial illness depending on its concentration.

Meanwhile Partial least squares (PLS) analysis displays scores for two factors called as Factor-1 and Factor-2 which retrieved from NIR spectroscopy data. The scores for both calibration and validation sets are provided by Fig. 12. Factor-1 scores is positive for microbial concentrations between 0.5%, 10% and 20% and negative for value between 50% and 100%. Factor-2 depicted a negative for concentrations between 0%, 5% and 100% and positive for 10%, 20% and 50%. In overall PLS's Factor-1 and Factor-2 abled to discriminate between the microbial concentrations into 4 categories of 0.5%;0.1 and 0.2%; 0% and 0.005%; 100%.
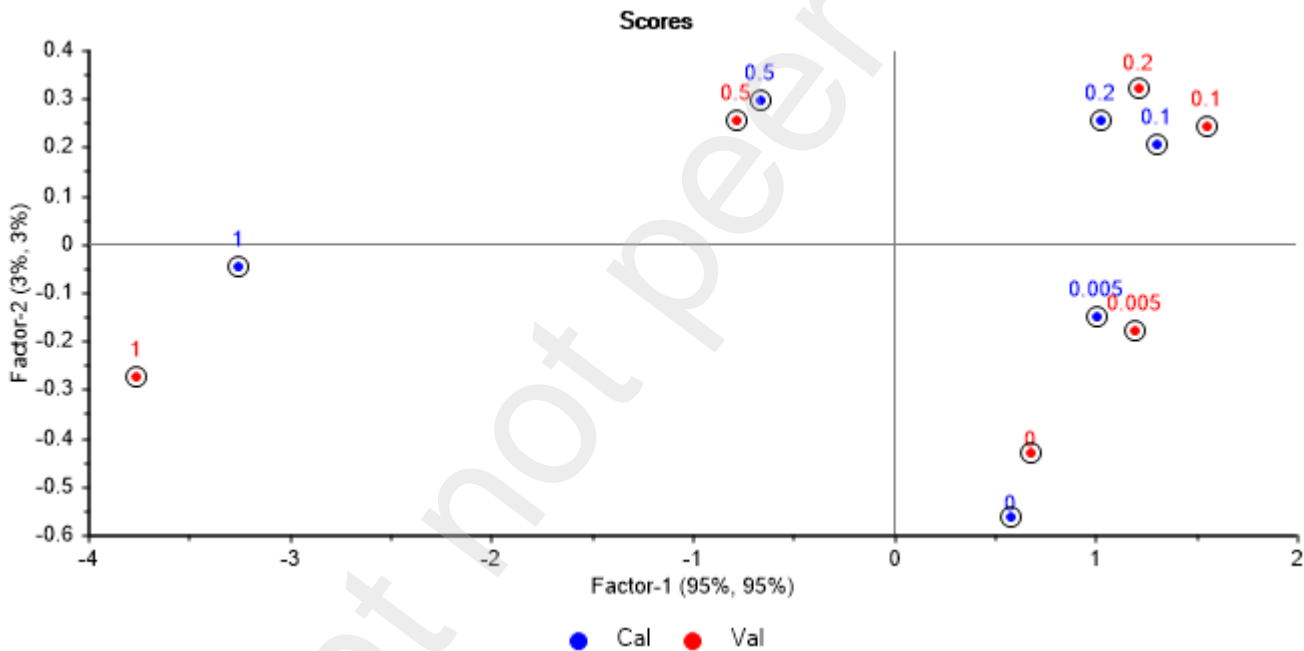
Fig. 12 PLS scores classification of S. boulardii using NIR spectroscopy data

Fig. 13 shows spectral data are gathered by NIR spectroscopy with a wavelength range between 900.81 and 1700.80 nm. The X-loading displays the model's weights for each wavelength. The X-loading plot may be used to discover significant spectral patterns associated with the abundance of S. boulardii. It is observed the range of wavelengths with the greatest loading are the most significant factor for determining the concentration. Similar to the X-loading, the Y-loading plot depicts the weights of each microbial concentration in the model. Based on Fig. 13, PLS can help build prediction models that can accurately estimate the concentration of S. boulardii based on NIR spectral data.
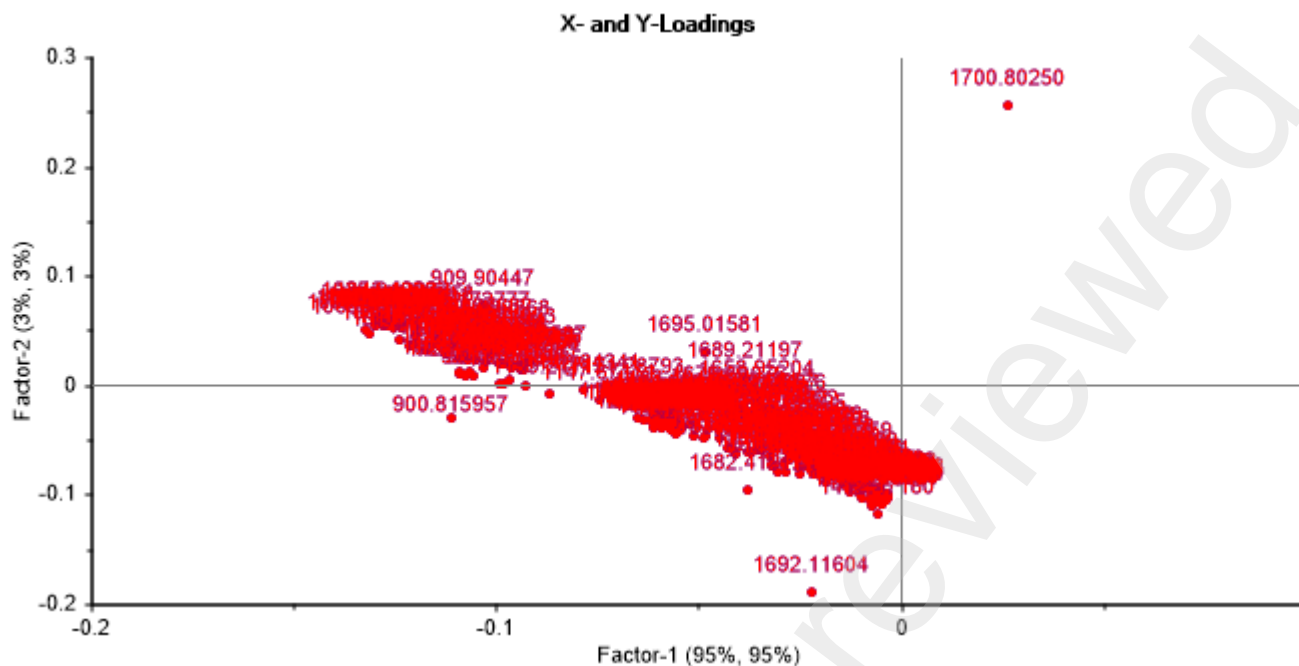
Fig. 13. X- and Y-loading for factor-1 and factor-2

*3.5 Correlation of NIR and DO's IoT based sensors Method*

Overall, IoT based sensor's DO parameter has the capability of classifying microbial based on its concentrations. In table 4, measurements of NIR trans-reflectance spectra in the limit range of 900–1700 nm from suspended microbial solutions indicate the presence of distinct absorption bands, notably around about 1500 nm. This band is mostly related to water absorption and O-H bonding; however, the effects of water absorption may be mitigated by measuring the trans-reflectance of liquid samples. This improves the ability to identify and differentiate microorganisms. Additionally, chemometrics aids in distinguishing and categorising microbial species. NIR spectroscopy measurements can also easily detect microorganism concentrations ranging from 50% to 100% with a response time of less than 10 seconds for scanning spectra absorption. The sensing range for scanning with test tube sample yeast is 1 mm through its optical window and is nearly gapless.

DO sensor measurement is the most important factor affecting the effect of yeast in water compare to TDS, EC, Ph, and temperature. This method of DO sensor measurement can detect yeast with a concentration of 50% to 100% of *S. boulardii*, the same as with NIR spectroscopy measurement. DO measurement has different response time, sensing range and limit detection range for detect yeast with NIR spectroscopy. Detection of yeast *S. boulardii* has been limited to 4-8 mg/L and set a long response time of more than 1 hour; additionally, the sensing range for a DO sensor measuring yeast in water is 9 cm. Table 5 shows summarize of NIR spectroscopy comparison method with DO

sensor. This proves NIR spectroscopy is a highly-sensitivity and effectively device to detect a microorganism concentration in water by validated with demonstrated with DO sensor. In chart Fig. 14, the value of the detection method's output will be compared as both methods' output for 50% and 100% microbial bacterial concentrations will have the same effect on the ability to detect yeast with different value unit of sensor.

Table 4 Comparison of method NIR spectroscopy with DO sensor with highly efficient techniques to detect yeast.

Name of detection method	S. boulardii concentration (%)	Significant Spectrum Wavelength output	Limit of detection	Response time (s)	Sensing range (mm)
NIR spectroscopy measurements	50%	1067 nm :0.357	900–1700 nm	< 10 second	1mm
	100%	1067 nm :0.121			
DO sensor measurement in water	50%	7.824 mg/L effect of acclimatization	4-8mg/L	> 1 hours	9 cm
	100%	6.288 mg/L effect of acclimatization			
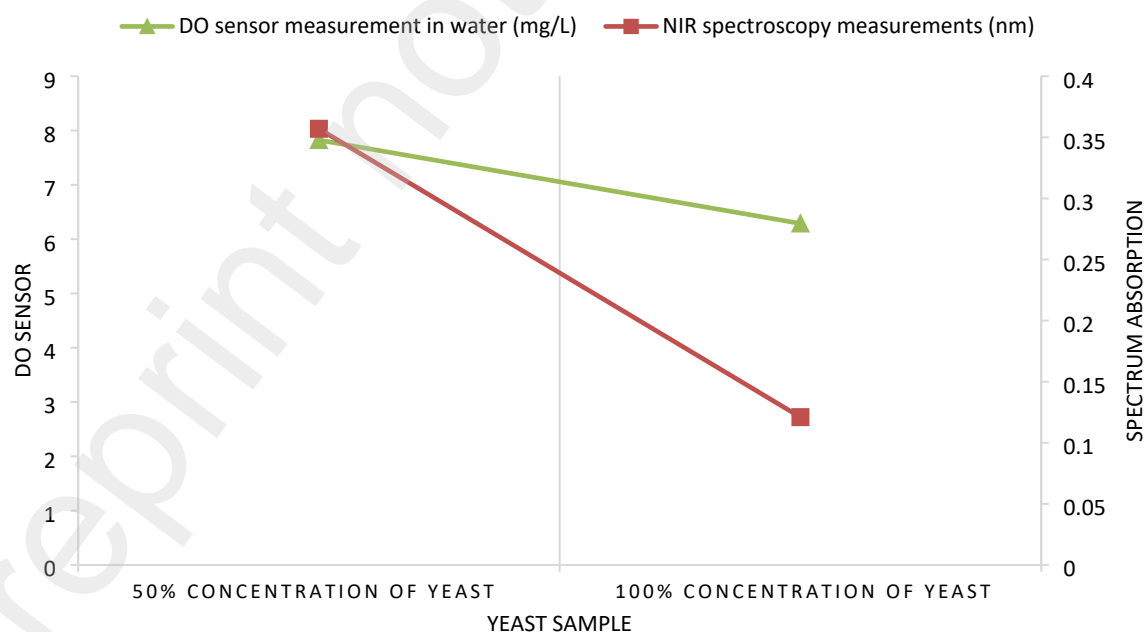
Fig. 14 Chart comparison data sample 50% and 100% concentration of S. boulardii for DO sensor and NIR spectroscopy

4. CONCLUSION

A new measurement approach to detect concentration of *S. boulardii* based on highly sensitive NIR spectroscopy emission is identified. NIR spectroscopy allowed an instant detection of *S. boulardii* in water within 900 to 1700 nm wavelength. The experiment found that spectroscopy exhibits specific pattern based on concentration of 10%, 20%, 50% and 100% which generated spectral absorbance of 0.723, 0.64, 0.357 and 0.121 correspondingly at 1067 nm wavelength. This finding is further validated by the DO sensor which demonstrates a rising of 8 mg/L after an hour of *S. boulardii 's* inoculation compared to 4 mg/L without inoculation and level back to normal after 5 hours. It can be inferred that the NIR spectroscopy sensor as an excellent option for microbial sensing in water.

ACKNOWLEDGEMENT

REFERENCES

[1] X. Yang *et al.*, "Label-free bacterial colony detection and viability assessment by continuous-wave terahertz transmission imaging," *J Biophotonics*, vol. 11, no. 8, Aug. 2018, doi: 10.1002/jbio.201700386.

[2] S. J. Park *et al.*, "Detection of microorganisms using terahertz metamaterials," *Sci Rep*, vol. 4, May 2014, doi: 10.1038/srep04988.

[3] R. Gente and M. Koch, "Monitoring leaf water content with THz and sub-THz waves," *Plant Methods*, vol. 11, no. 1. BioMed Central Ltd., Jul. 01, 2015. doi: 10.1186/s13007-015-0057-7.

[4] D. A. Burns, E. W. Ciurczak, C. A. Anderson, and J. K. Drennen, "Handbook of Near-Infrared Analysis Third Edition 30 Pharmaceutical Applications of Near-Infrared Spectroscopy," 2008.

[5] G. Valušis, A. Lisauskas, H. Yuan, W. Knap, and H. G. Roskos, "Roadmap of terahertz imaging 2021," *Sensors*, vol. 21, no. 12. MDPI AG, Jun. 02, 2021. doi: 10.3390/s21124092.

[6] S. J. Park *et al.*, "Detection of microorganisms using terahertz metamaterials," *Sci Rep*, vol. 4, May 2014, doi: 10.1038/srep04988.

[7] Quantitative polymerase chain reaction (Q-PCR) and fluorescent in situ hybridization (FISH) detection of soilborne pathogen Sclerotium rolfsii. Milner, H., et al., et al. 2019, Applied Soil Ecology, 136, pp. 86-92.

[8] Engvall, E. (2010). The ELISA, enzyme-linked immunosorbent assay. In *Clinical Chemistry* (Vol. 56, Issue 2, pp. 319–320). https://doi.org/10.1373/clinchem.2009.127803

[9] Zaqout, S., Becker, L. L., & Kaindl, A. M. (2020). Immunofluorescence Staining of Paraffin Sections Step by Step. *Frontiers in Neuroanatomy*, *14*. https://doi.org/10.3389/fnana.2020.582218

[10] Levsky, J. M., & Singer, R. H. (2003). Fluorescence in situ hybridization: Past, present and future. In *Journal of Cell Science* (Vol. 116, Issue 14, pp. 2833–2838). https://doi.org/10.1242/jcs.00633

[11] *Temporal patterns of airborne Phytophthora spp. in a woody plant nursery area detected using real-time PCR*. Migliorini, D., et al., et al. 1, 2019, Aerobiologia, 35(2), Vol. 31, pp. 201-214.

[12] Call, D. R., Borucki, M. K., & Loge, F. J. (2003). Detection of bacterial pathogens in environmental samples

using DNA microarrays. In *Journal of Microbiological Methods* (Vol. 53, Issue 2, pp. 235–243). Elsevier. https://doi.org/10.1016/S0167-7012(03)00027-7

[13]   Henard, C. A., Franklin, T. G., Youhenna, B., But, S., Alexander, D., Kalyuzhnaya, M. G., & Guarnieri, M. T. (2018). Biogas Biocatalysis: Methanotrophic Bacterial Cultivation, Metabolite Profiling, and Bioconversion to Lactic Acid. *Frontiers in Microbiology*, *9*. https://doi.org/10.3389/fmicb.2018.02610.

[14]   Marchetti, C. F., Ugena, L., Humplík, J. F., Polák, M., Čavar Zeljković, S., Podlešáková, K., Fürst, T., de Diego, N., & Spíchal, L. (2019). A Novel Image-Based Screening Method to Study Water-Deficit Response and Recovery of Barley Populations Using Canopy Dynamics Phenotyping and Simple Metabolite Profiling. *Frontiers in Plant Science*, *10*. https://doi.org/10.3389/fpls.2019.01252.

[15]   Cambré, A., & Aertsen, A. (2020). Bacterial Vivisection: How Fluorescence-Based Imaging Techniques Shed a Light on the Inner Workings of Bacteria. *Microbiology and Molecular Biology Reviews*, *84*(4). https://doi.org/10.1128/mmbr.00008-20

[16]   Alvarez-Ordóñez, A., Mouwen, D. J. M., López, M., & Prieto, M. (2011). Fourier transform infrared spectroscopy as a tool to characterize molecular composition and stress response in foodborne pathogenic bacteria. In *Journal of Microbiological Methods* (Vol. 84, Issue 3, pp. 369–378). https://doi.org/10.1016/j.mimet.2011.01.009

[17]   Park, S. J., Hong, J. T., Choi, S. J., Kim, H. S., Park, W. K., Han, S. T., Park, J. Y., Lee, S., Kim, D. S., & Ahn, Y. H. (2014). Detection of microorganisms using terahertz metamaterials. *Scientific Reports*, *4*. https://doi.org/10.1038/srep04988

[18]   Z. Kovacs, J. Muncan, P. Veleva, M. Oshima, S. Shigeoka, and R. Tsenkova, "Aquaphotomics for monitoring of groundwater using short-wavelength near-infrared spectroscopy," *Spectrochim Acta A Mol Biomol Spectrosc*, vol. 279, Oct. 2022, doi: 10.1016/j.saa.2022.121378.

[19]   P. Krepelka, F. Pérez-Rodríguez, and K. Bartusek, "BACTERIAL PATTERN IDENTIFICATION IN NEAR-INFRARED SPECTRUM," *Informatyka, Automatyka, Pomiary w Gospodarce i Ochronie Środowiska*, vol. 4, no. 3, pp. 58–60, Sep. 2014, doi: 10.5604/20830157.1121369.

[20]   T. D. A. Petya Veleva-Doneva, "Detection of bacterial contamination in milk using NIR spectroscopy and two classification method".

[21]   F. A. K. S. R. Zsanett Bodor, "Application of Near Infrared Spectroscopy and Classical Analytical Methods For the Evaluation of Hungarian Honey".

[22]   A. A. Gowen, Y. Tsuchisaka, C. O'Donnell, and R. Tsenkova, "Investigation of the Potential of Near Infrared Spectroscopy for the Detection and Quantification of Pesticides in Aqueous Solution," *Am J Analyt Chem*, vol. 02, no. 08, pp. 53–62, 2011, doi: 10.4236/ajac.2011.228124.

[23]   A. O' Reilly, R. Coffey, A. Gowen, and E. Cummins, "Evaluation of near-infrared chemical imaging for the prediction of surface water quality parameters," *Int J Environ Anal Chem*, vol. 95, no. 5, pp. 403–418, Apr. 2015, doi: 10.1080/03067319.2015.1025222.

[24]   Z. Kovacs, J. Muncan, P. Veleva, M. Oshima, S. Shigeoka, and R. Tsenkova, "Aquaphotomics for monitoring of groundwater using short-wavelength near-infrared spectroscopy," *Spectrochim Acta A Mol Biomol Spectrosc*, vol. 279, Oct. 2022, doi: 10.1016/j.saa.2022.121378.

[25]   K. B. Beć, J. Grabska, and C. W. Huck, "Near-infrared spectroscopy in bio-applications," *Molecules*, vol. 25, no. 12. MDPI AG, Jun. 01, 2020. doi: 10.3390/molecules25122948.

[26]   Siew, S. W., Musa, S. M., Sabri, N. 'Azyyati, Farida Asras, M. F., & Ahmad, H. F. (2023). Evaluation of pre-treated healthcare wastes during COVID-19 pandemic reveals pathogenic microbiota, antibiotics residues, and antibiotic resistance genes against beta-lactams. *Environmental Research*, *219*. https://doi.org/10.1016/j.envres.2022.115139

[27]   Karthikeyan, S., Levy, J. I., de Hoff, P., Humphrey, G., Birmingham, A., Jepsen, K., Farmer, S., Tubb, H. M., Valles, T., Tribelhorn, C. E., Tsai, R., Aigner, S., Sathe, S., Moshiri, N., Henson, B., Mark, A. M., Hakim, A., Baer, N. A., Barber, T., … Knight, R. (2022). Wastewater sequencing reveals early cryptic SARS-CoV-2 variant transmission. *Nature*, *609*(7925), 101–108. https://doi.org/10.1038/s41586-022-05049-6

[28]   Wei, S. S., Yen, C. M., Marshall, I. P. G., Hamid, H. A., Kamal, S. S., Nielsen, D. S., & Ahmad, H. F. (2022). Gut microbiome and metabolome of sea cucumber (Stichopus ocellatus) as putative markers for monitoring the marine sediment pollution in Pahang, Malaysia. *Marine Pollution Bulletin*, *182*. https://doi.org/10.1016/j.marpolbul.2022.114022

[29]   Tay, D. D., Siew, S. W., Shamzir Kamal, S., Razali, M. N., & Ahmad, H. F. (2022). ITS1 amplicon sequencing of feline gut mycobiome of Malaysian local breeds using Nanopore Flongle. *Archives of Microbiology*, *204*(6).

https://doi.org/10.1007/s00203-022-02929-3

[30]   A. G. Császár *et al.*, "On equilibrium structures of the water molecule," *Journal of Chemical Physics*, vol. 122, no. 21, Jun. 2005, doi: 10.1063/1.1924506.

[31]   S. M. Z. Hossain and N. Mansour, "Biosensors for on-line water quality monitoring–a review," *Arab Journal of Basic and Applied Sciences*, vol. 26, no. 1. Taylor and Francis Ltd., pp. 502–518, Jan. 02, 2019. doi: 10.1080/25765299.2019.1691434.

[32]   N. nan Song *et al.*, "A novel electrochemical biosensor for the determination of dopamine and ascorbic acid based on graphene oxide /poly(aniline-co-thionine) nanocomposite," *Journal of Electroanalytical Chemistry*, vol. 873, Sep. 2020, doi: 10.1016/j.jelechem.2020.114352.

[33]   I. M. Hakimi and Z. Jamil, "Development of Water Quality Monitoring Device Using Arduino UNO," *IOP Conf Ser Mater Sci Eng*, vol. 1144, no. 1, p. 012064, May 2021, doi: 10.1088/1757-899x/1144/1/012064.

[34]   jill seladi-schulman, "what are bacteria and what do they do," *MedicalNewToday*, 2019.